

OPTICALLY STIMULATED LUMINESCENCE OF THE β -IRRADIATED $\text{Li}_2\text{B}_4\text{O}_7:\text{Cu}$, Eu GLASS

B.V. PADLYAK¹, I.I. KINDRAT², K. SZUFA³, A. MANDOWSKI³

¹O.G. Vlokh Institute of Physical Optics of the Ivan Franko National University of Lviv,
23 Dragomanov Str., 79-005 Lviv, Ukraine

²University of Zielona Góra, Institute of Physics, Division of Spectroscopy of Functional Materials,
4a Szafrana Str., 65-516 Zielona Góra, Poland

³Jan Długosz University in Częstochowa, Faculty of Science & Technology, Institute of Physics,
13/15 Armii Krajowej Str., 42-200 Częstochowa, Poland

Received: 13.03.2025

Abstract. The $\text{Li}_2\text{B}_4\text{O}_7:\text{Cu}$, Eu glass has been investigated as a potential active element in optically stimulated luminescence (OSL) dosimetry. For this purpose, the dependence of the integrated total infrared OSL (IR-OSL) signal on the dose of β -irradiation (the $^{90}\text{Sr}/^{90}\text{Y}$ β -source) and the IR-OSL decay curves were obtained and analyzed. It was established that the IR-OSL intensity becomes sublinear at very high radiation doses, while the OSL decay does not belong to the first and second-order kinetics and is described by the sum of three exponential components.

Keywords: $\text{Li}_2\text{B}_4\text{O}_7:\text{Cu}$, Eu glass, β -irradiation, optically stimulated luminescence, dose dependence, decay curve

UDC: 535.37

DOI: 10.3116/16091833/Ukr.J.Phys.Opt.2025.03001

1. Introduction

In recent decades, the phenomenon of optically stimulated luminescence (OSL) in various materials has been intensively studied with the prospect of its widespread application in radiation protection dosimetry. The basis of OSL dosimeters is a working element in which stable radiation centers are formed under X, γ , β , and other types of ionizing irradiation, which can be centers of luminescence upon optical excitation [1,2]. An interesting feature of OSL is the possibility of its use in medical 2D and 3D dosimeters for radiotherapy [3,4], which stimulates the active search and research of new effective crystalline and glassy (or vitreous) OSL materials.

The borate glassy compounds are promising dosimetry materials based on thermoluminescence (TL) and OSL phenomena [5,6]. In addition to other types of ionizing radiation, the borate crystalline and glassy compounds are also sensitive to neutron irradiation due to the presence of the ^{10}B boron isotope (natural abundance – 19.6 %) with a large interaction cross-section that allows the manufacture of OSL dosimeters for a wide range of radiation exposure, including neutrons [7–10]. It should be noted that using the borate compounds for neutron OSL dosimeters is especially important. In particular, the dosimeters can be used to monitor neutron radiation in nuclear power plants and in defense to determine the dose of neutron exposure of military pilots during high-altitude flights [11]. Besides this, the OSL dosimeters are also very promising for monitoring various types of cosmic radiation on orbital stations and during long-time space flights [12].

Currently, the mechanisms of TL and OSL have not been fully investigated, even for well-known dosimetric materials that are already in use. A key issue in the development of materials for dosimetry is the presence after their irradiation of a high concentration of stable radiation centers captured by structural defects (traps), which can be reproduced repeatedly after their exposure under the influence of heat (during the TL phenomenon) or light (during OSL phenomenon). As an example, we can cite the work [13] in which an OSL dosimeter based on phosphate glass activated by Ag^+ ions is proposed to obtain 2D and 3D images of the distribution of the absorbed dose of X-ray radiation. Although phosphate glasses activated by Ag^+ ions have been used in OSL dosimetry for a relatively long time, their intensive research is still ongoing. This indicates that phosphate glass does not solve all the problems of OSL dosimetry and that it is necessary to continue researching the nature and mechanisms of OSL in new, more promising materials. A number of publications are devoted to the research of OSL in various materials in the form of polycrystalline powders, single crystals, and nanocomposites. For example, in [3] the possibility of obtaining spectroscopic information about the radiation field when using OSL on F_2^+ and F_3^+ colour centres in LiF single crystals was considered. It turned out that 2D radiation OSL dosimeters can also be implemented on the classical TL dosimetric material LiF:Mg, Cu, P in a powder form [4]. The authors of [4] demonstrated a clear distribution of the dose from a $^{90}\text{Sr}/^{90}\text{Y}$ β -source along the profile of a pressed disc made of LiF:Mg,Cu, P with a diameter of 8 mm and a thickness of 0.5 mm in two mutually perpendicular directions. The OSL properties of the $\text{MgGa}_2\text{O}_4:\text{Mn}^{2+}$ phosphor were published in [14].

As was noted above, the borate (glassy and crystalline) compounds are also promising materials for OSL dosimetry since they can be used for neutron dosimetry due to the content of the ^{10}B isotope. Therefore, in recent years, studies of the effectiveness of OSL in borates have been carried out on vitreous [5,6] and polycrystalline powdered samples [7–9], as well as on glass ceramics [10]. The articles [5–10] established the prospects of borate compounds for OSL dosimetry. The above short list of OSL studies realized recently in various materials, including borates, shows that such studies should be continued, particularly on the borate glasses and glass ceramics, including glass nanoceramics (i.e., crystalline nanoparticles in glass matrix).

Borate glasses with different basic compositions can be obtained by relatively cheap technology and allow the addition in their structure of a higher amount of luminescent ions in comparison with corresponding crystalline compounds. Therefore, borate glasses are promising materials for OSL dosimetry. At present, there has been developed a very simple technology of borate glasses with basic chemical compositions close to their well-known crystalline analogs. As a result, a number of borate glasses with different basic compositions doped with rare-earth elements were obtained. The local and electron structure, as well as the spectroscopic and optical-luminescent properties of the obtained borate glasses doped with rare-earth elements (Ce, Nd, Dy, Tb, Er, Eu, Gd, Yb, Sm, Tm), were detailed studied and published in a series of our articles [15–26]. In the following articles [27–35], an increase (in some cases significant) of the intensity and quantum yield of the photoluminescence (PL) of rare-earth ions in the borate glasses was noted when they were co-doped with silver (Ag) in the amount of 2.0 mol.%. The observed increase of the intensity and quantum yield of PL in borate glasses co-doped with rare-earth elements and Ag is due to the excitation energy

transfer from the Ag^+ impurity ions and molecular-like silver nanoclustered aggregates to rare-earth ions and to the effects induced by the surface plasmon resonance (SPR) of the silver (Ag^0) metallic nanoparticles, which are localized in the matrix of borate glasses.

During the last years, glasses of high optical quality with $\text{Li}_2\text{B}_4\text{O}_7$ basic composition, co-doped with rare-earth (Eu, Sm, Er) and transition (Cu, Mn) elements in the amount of 1.0 mol.%, have been obtained. The local structure, spectroscopic, and optical-luminescent properties of the obtained glasses were thoroughly examined in our articles [36–40]. In particular, possible excitation energy transfer processes $\text{Sm}^{3+} \rightarrow \text{Mn}^{2+}$, Mn^{3+} , and $\text{Mn}^{2+} \rightarrow \text{Mn}^{3+}$ in the $\text{Li}_2\text{B}_4\text{O}_7:\text{Mn}$, Sm glass and $\text{Eu}^{3+} \leftrightarrow \text{Mn}^{2+}$, Mn^{3+} , and $\text{Mn}^{2+} \rightarrow \text{Mn}^{3+}$ in the $\text{Li}_2\text{B}_4\text{O}_7:\text{Mn}$, Eu glass are considered in [37,38]. The absence of characteristic Er^{3+} photoluminescence bands in the $\text{Li}_2\text{B}_4\text{O}_7:\text{Mn}$, Er glass in [39] is explained by mechanisms of excitation energy transfer from Er^{3+} to Mn^{2+} and Mn^{3+} ions. Based on the spectroscopic studies of the $\text{Li}_2\text{B}_4\text{O}_7:\text{Cu}$, Sm glass in [40] it was shown that the observed changes in PL intensity, shortening of the Sm^{3+} lifetime and prolongation of the Cu^+ lifetime are caused by energy transfer $\text{Sm}^{3+} \rightarrow \text{Cu}^+$ and re-absorption of the Sm^{3+} emission by Cu^{2+} non-luminescent ions.

Let's briefly consider the main results of structural and spectroscopic characterization of the $\text{Li}_2\text{B}_4\text{O}_7:\text{Cu}$, Eu glass, which is investigated in this article by the OSL technique after β -irradiation. Results of detailed XRD studies and analysis of the local structure of the $\text{Li}_2\text{B}_4\text{O}_7:\text{Cu}$, Eu glass are published in our article [36]. The EPR and optical absorption, emission, and photoluminescence excitation show that the Cu impurity is incorporated into the $\text{Li}_2\text{B}_4\text{O}_7:\text{Cu}$, Eu glass as Cu^{2+} ($3d^9$) and Cu^+ ($3d^{10}$) ions. The Cu^{2+} ions in $\text{Li}_2\text{B}_4\text{O}_7:\text{Cu}$, Eu glass show characteristic EPR and optical absorption spectra. The spin Hamiltonian parameters of the Cu^{2+} EPR spectrum were determined by best fitting the simulated EPR spectrum to the experimental spectrum, recorded at $T = 295$ K. Optical absorption spectrum of the $\text{Li}_2\text{B}_4\text{O}_7:\text{Cu}$, Eu glass was analyzed and interpreted. The optical band gap and Urbach energy of the $\text{Li}_2\text{B}_4\text{O}_7:\text{Cu}$, Eu glass were evaluated. Photoluminescence spectra of the $\text{Li}_2\text{B}_4\text{O}_7:\text{Cu}$, Eu glass reveal a broad blue emission band of the Cu^+ ($3d^9 4s^1 \rightarrow 3d^{10}$ transition) and narrow emission bands in the orange-red range of the Eu^{3+} ($4f^6$) ions belonging to the ${}^5\text{D}_0 \rightarrow {}^7\text{F}_j$ ($J = 0 - 4$) transitions with characteristic decay kinetics. Two energy transfer mechanisms in the $\text{Li}_2\text{B}_4\text{O}_7:\text{Cu}$, Eu glass are proposed in [36]. The first mechanism is related to UV-violet excitation energy transfer from the Eu^{3+} ions to the Cu^+ ions. The second stronger mechanism is related to energy transfer from the Eu^{3+} ions to the Cu^{2+} ions.

As was noted above, the OSL in borate crystals and glasses has been relatively weakly studied and published only in several articles, particularly in [5–10,41]. For example, in the $\text{Li}_2\text{B}_4\text{O}_7:\text{Ag}$ single crystal irradiated by X-rays at room temperature, an OSL band with a maximum of 270 nm was recorded under continuous excitation with a wavelength of 400 nm [41]. However, until now, the OSL in the $\text{Li}_2\text{B}_4\text{O}_7$ glass, co-doped with rare-earth and transitional metals, has not been studied in detail. Therefore, such research should be continued to study the nature and mechanisms of OSL in borate glasses co-doped with rare-earth and transitional elements and evaluate their potential applications in modern OSL dosimetry. In this article firstly are presented the results of OSL studies of the $\text{Li}_2\text{B}_4\text{O}_7:\text{Cu}$, Eu glass after β -irradiation at room temperature in a wide dose range.

2. Experimental details

The samples of borate glasses have been obtained using the method described in detail in [36,42]. Optically stimulated luminescence was registered on the obtained $\text{Li}_2\text{B}_4\text{O}_7:\text{Cu}$, Eu

samples, which were cut and polished to a size of $(10 \times 5 \times 2)$ mm³. Before the OSL measurements, the Li₂B₄O₇:Cu, Eu sample was irradiated with a ⁹⁰Sr/⁹⁰Y β-source with an activity of 2.9 GBq and a dose rate of 0.069 Gy/s. The irradiation process was carried out in the dark. The OSL registration was made using the OSL Helios reader (Zero-Rad). The reader used integrated H7360 (Hamamatsu) photon counting modules with quartz windows. The obtained data were collected by a dedicated electronic system, which sent them to a computer. The reader is also equipped with an additional photosensor used to control the emission of LEDs. The OSL measurements were performed in the continuous wave OSL (CW-OSL) mode, where the sample is illuminated with light of constant intensity during the measurement.

The reader was equipped with fifteen IR diodes for the infrared OSL (IR-OSL) measurements, which stimulated the samples in the range of 840 – 870 nm (peak 850 nm). The light emitted by LEDs was additionally filtered by the RG715 (Schott) filters with 3 mm thickness. Luminescence detection was performed in the 300 – 600 nm range with a maximum of about 500 nm using 2.5 mm BG39 (Schott) filters.

3. Experimental results and their analysis

3.1. Analysis of the infrared optically stimulated luminescence of the β-irradiated Li₂B₄O₇:Cu, Eu glass

The infrared optically stimulated luminescence (IR-OSL) dose response of the β-irradiated Li₂B₄O₇:Cu, Eu glass is presented in Fig. 1. As one can see, the linear fit given by the red curve is not appropriate in this case, and the dose response exhibits an apparent sublinear behavior. To characterize this dependence, the observed line was fitted using the following power law:

$$S(D) = S_0 \left(\frac{D}{D_0} \right)^\gamma, \quad (1)$$

where S is a total OSL signal integrated into a given rangem and D is the dose of β-radiation, S_0 is the integrated OSL signal measured for the D_0 dose. In our case, value $D_0 = 100$ Gy.

The γ coefficient specifies the nonlinearity of the observed dependence. For $\gamma < 1$, the dependence is sublinear, but for $\gamma > 1$, the dependence is superlinear. Fit of the dose response data to Eq. (1) confirms the sublinearity, which is characterized by the coefficient

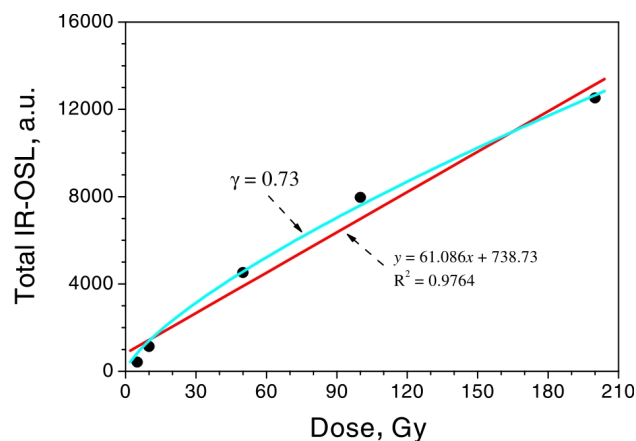


Fig. 1. The dependence of the integrated total IR-OSL signal of Li₂B₄O₇:Cu, Eu vs. the dose of β-irradiation, fitted by the linear regression (red curve) and the power law formula (blue curve). (Color online).

$\gamma = 0.73$. The obtained resulting plot is given by the blue curve in Fig. 1, which presents the integrated total IR-OSL signal of $\text{Li}_2\text{B}_4\text{O}_7\text{:Cu, Eu}$ glass vs the dose of the β -irradiation with the fitted power-law dependence given by Eq. (1).

3.2. Analysis of the IR-OSL decay curves (CW-OSL) for $\text{Li}_2\text{B}_4\text{O}_7\text{:Cu, Eu}$ glass

The long-lasting OSL decay results from the optical release of charge carriers from deep traps. The mechanism of radiative recombination depends on various material parameters [1]. Below, some basic mechanisms of radiative recombination are considered. The approximate kinetic analysis is based on quasi-equilibrium conditions [1,2].

1. The simplest case is the first-order kinetic mechanism. It relates to the case of a single active trap level when de-trapping of charge carriers due to optical stimulation takes place without re-trapping. The luminescence intensity J_{OSL} is directly proportional to the rate at which the number N of charge carriers in traps decreases, given by:

$$J_{OSL}(t) = -(dN/dt). \quad (2)$$

The rate of decay is proportional to the number N of charge carriers in traps remaining at time t , given by:

$$dN/dt = -\alpha N, \quad (3)$$

where α is constant. Solving the Eq. (3) and substituting the solution into the Eq. (2) was obtained:

$$J_{OSL}(t) = A \exp\left(-t/\tau\right), \quad (4)$$

where A and $\tau = 1/\alpha$ are constants, particularly the τ may be interpreted as a characteristic lifetime. Therefore, by plotting $\ln(J_{OSL})$ vs. time (t), we get a straight line. Unfortunately, the fit does not work in our case, as shown in Fig. 2 for $\text{Li}_2\text{B}_4\text{O}_7\text{:Cu, Eu}$ glass, β -irradiated by a dose of 200 Gy. The exponential fit defined by Eq. (4) is done in data range from 1 to 4 s. The characteristic average lifetime value for this range is $\tau = 1.87$ s.

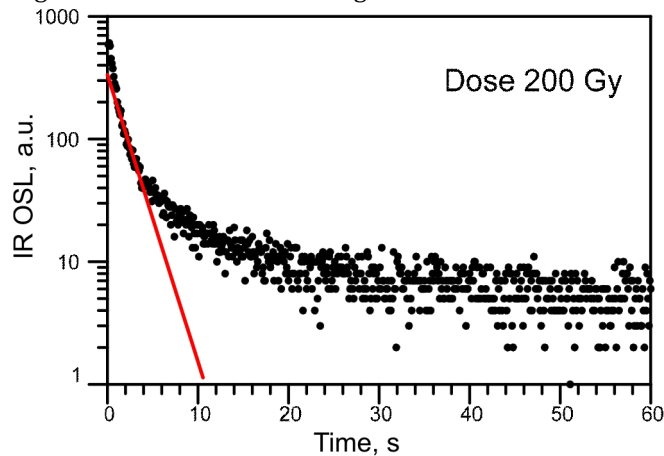


Fig. 2. The IR-OSL decay in the $\text{Li}_2\text{B}_4\text{O}_7\text{:Cu, Eu}$ glass, β -irradiated by a dose of 200 Gy. The red line presents the exponential fit defined by Eq. (4). (Color online).

2. The next case is the case with strong re-trapping. A charge carrier excited by the stimulation light from a trap level to the transport band (i.e., the conduction or the valence band) has a high probability of returning to the same trap level. In this case, the kinetic equation is:

$$\frac{dN}{dt} = -\alpha N^2 \quad (5)$$

where α is constant. This is the so-called second-order equation. Solving the Eq. (5) and substituting the solution into the Eq. (2) was obtained:

$$J_{OSL}(t) = \frac{A}{(1 + \delta t)^2}, \quad (6)$$

where A and $\delta \propto \alpha$ are constants. Rearranging the last equation, we get the following relation:

$$\frac{1}{\sqrt{J_{OSL}}} = \frac{1}{\sqrt{A}} + \frac{\delta}{\sqrt{A}} t, \quad (7)$$

The plots of the $1/\sqrt{J_{OSL}}$ value vs. time (t) are shown in Figs. 3 and 4 for the β -irradiation doses of 100 Gy and 200 Gy, respectively. The obtained plots are not straight lines, so the OSL mechanism is not the second-order mechanism.

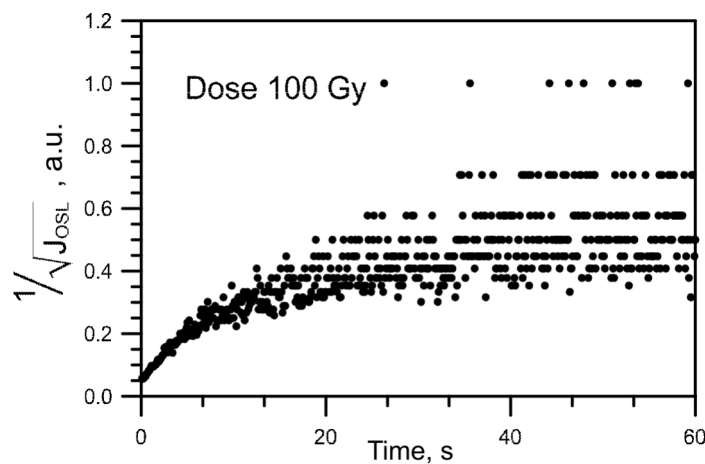


Fig. 3. The plot to check the second-order recombination mechanism for the sample irradiated with 100 Gy.

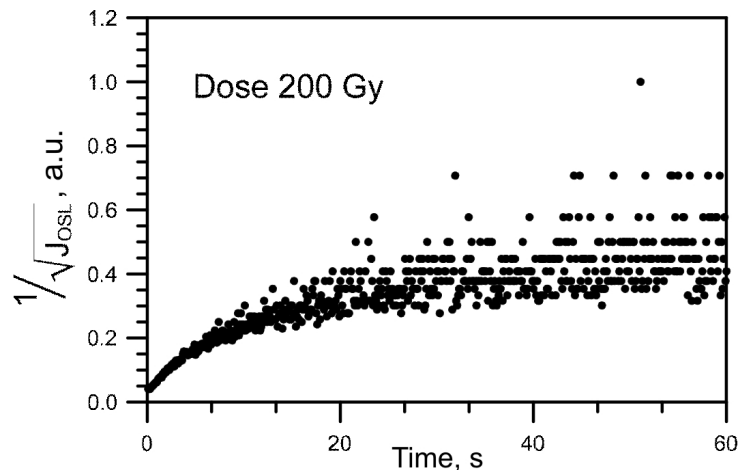


Fig. 4. The plot to check the second order-recombination mechanism for the sample irradiated with 200 Gy.

3. When several trap levels are active in the same temperature and comparable time scale, it is often considered that the luminescence decay consists of several first-order components, i.e.:

$$J_{OSL}(t) = \sum_{i=1}^p A_i \exp\left(-t/\tau_i\right). \quad (8)$$

The three-exponential fit of the OSL decay is shown in Figs. 5 and 6 for the β -irradiation doses of 100 Gy and 200 Gy, respectively. Three is the minimum number of exponential components that gives a good quality fit. Thus, the OSL decay of the $\text{Li}_2\text{B}_4\text{O}_7:\text{Cu}, \text{Eu}$ glass does not belong purely to the first and second-order recombination mechanisms and is described by the sum of three exponential components, suggesting a continuous distribution of traps in the investigated glass.

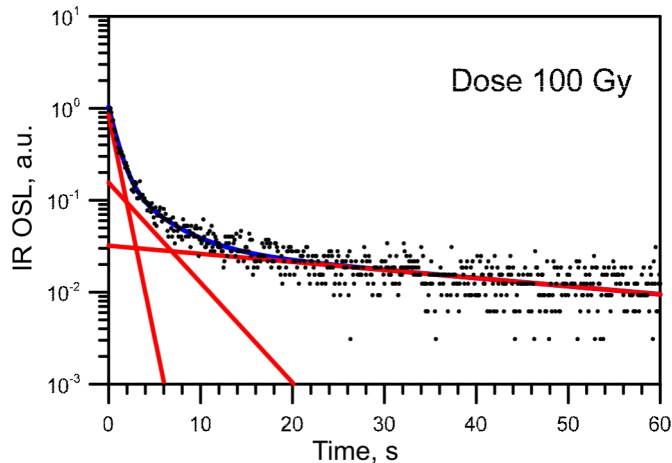


Fig. 5. Three-component exponential fit for the OSL decay of the $\text{Li}_2\text{B}_4\text{O}_7:\text{Cu}, \text{Eu}$ glass irradiated with a dose of 100 Gy. The red curves represent individual exponents. The blue curve represents the summarized curve defined by Eq. (8). The determined lifetimes are: $\tau_1 = 0.85$ s, $\tau_2 = 4.0$ s, and $\tau_3 = 49.2$ s. (Color online).

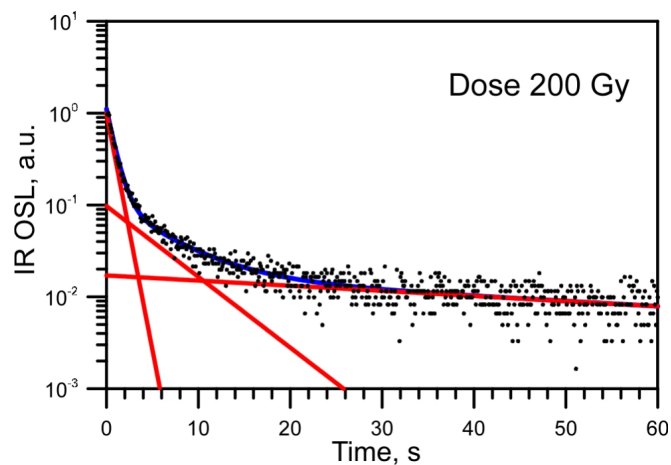


Fig. 6. Three-component exponential fit for the OSL decay of the $\text{Li}_2\text{B}_4\text{O}_7:\text{Cu}, \text{Eu}$ glass irradiated with a dose of 200 Gy. The red curves represent individual exponents. The blue curve represents the summarized curve defined by Eq. (8). The determined lifetimes are: $\tau_1 = 0.85$ s, $\tau_2 = 5.5$ s, and $\tau_3 = 70.2$ s. (Color online).

Based on the presented results, one can suppose that the OSL mechanisms in the $\text{Li}_2\text{B}_4\text{O}_7:\text{Cu}, \text{Eu}$ glasses are related to Cu and Eu centers and the energy transfer between them. The specific models and mechanisms of OSL in the $\text{Li}_2\text{B}_4\text{O}_7:\text{Cu}, \text{Eu}$ glasses need more detailed studies, particularly the OSL studies of lithium tetraborate glasses, co-doped with other elements of transitional and rare-earth groups.

4. Conclusions

The OSL of β -irradiated $\text{Li}_2\text{B}_4\text{O}_7\text{:Cu, Eu}$ glass containing 1.0 mol.% CuO and Eu_2O_3 is investigated and analyzed. Based on the presented results, one can state the following:

- The integrated total IR-OSL signal of $\text{Li}_2\text{B}_4\text{O}_7\text{:Cu, Eu}$ glass vs dose of β -irradiation is satisfactory fitted by a power law with the value of γ coefficient equals 0.73 that is characteristic for a sublinear dependence.
- Three basic mechanisms of radiative recombination, which can lead to long-lasting OSL decay in the $\text{Li}_2\text{B}_4\text{O}_7\text{:Cu, Eu}$ glass, are considered and analyzed. The OSL decay of the $\text{Li}_2\text{B}_4\text{O}_7\text{:Cu, Eu}$ glass does not follow purely first and second-order kinetics and is best described by the sum of three exponential components.
- Based on the OSL decay, a mechanism of optical release of charge carriers from deep traps, which are continuously distributed in the glass network, is proposed.

Acknowledgements. This work has been supported by the Ministry of Education and Science of Ukraine in the framework of scientific project # 0122U001833. The authors would like to thank Dr. Sci. V.T. Adamiv and M.Sc. I.M. Teslyuk from the O.G. Vlokh Institute of Physical Optics of the Ivan Franko National University of Lviv for samples synthesis and preparation. This work was partly supported (KS and AM) by research project # 2014/15/N/ST10/05148 from the Polish National Science Centre.

References

1. Yukihiro, E. G., & McKeever, S. W. S. (2011). *Optically Stimulated Luminescence. Fundamentals and Applications*. Wiley.
2. Chen, R., & McKeever, S. W. S. (1997). *Theory of Thermoluminescence and Related Phenomena*. World Scientific Publishing.
3. Bilski, P., Marczevska, B., Gieszczyk, W., Kłosowski, M., Naruszewicz, M., Sankowska, M., & Kodaira, S. (2019). Fluorescent imaging of heavy charged particle tracks with LiF single crystals. *Journal of Luminescence*, 213, 82–87.
4. Sądziel, M., Bilski, P., Kłosowski, M., & Sankowska, M. (2020). A new approach to the 2D radiation dosimetry based on optically stimulated luminescence of LiF:Mg,Cu,P. *Radiation Measurements*, 133, 106293.
5. Barrera, G. R., Souza, L. F., Novais, A. L. F., Caldas, L. V. E., Abreu, C. M., Machado, R., Sussuchi, E. M., & Souza, D. N. (2019). Thermoluminescence and optically stimulated luminescence of $\text{PbO-H}_3\text{BO}_3$ and $\text{PbO-H}_3\text{BO}_3\text{-Al}_2\text{O}_3$ glasses. *Radiation Physics and Chemistry*, 155, 150–157.
6. Hegde, V., Prabhu, N., Wagh, A., Sayyed, M. I., Agar, O., & Kamath, S. D. (2019). Influence of 1.25 MeV gamma rays on optical and luminescent features of Er^{3+} doped zinc bismuth borate glasses. *Results in Physics*, 12, 1762–1769.
7. Souza, L. F., Novais, A. L. F., Antonio, P. L., Caldas, L. V. E., & Souza, D. N. (2019). Luminescent properties of $\text{MgB}_4\text{O}_7\text{:Ce, Li}$ to be applied in radiation dosimetry. *Radiation Physics and Chemistry*, 164, 108353.
8. França, L. V. S., & Baffa, O. (2020). Boosted UV emission on the optically and thermally stimulated luminescence of $\text{CaB}_6\text{O}_{10}\text{:Gd, Ag}$ phosphors excited by X-rays. *Applied Materials Today*, 21, 100829.
9. Ozdemir, A., Altunal, V., Guckan, V., Kurt, K., & Yegingil, Z. (2021). Luminescence characteristics of newly-developed $\text{MgB}_4\text{O}_7\text{:Ce}^{3+}, \text{Na}^+$ phosphor as an OSL dosimeter. *Journal of Alloys and Compounds*, 865, 158498.
10. Kitagawa, Y., Yukihiro, E. G., & Tanabe, S. (2021). Development of Ce^{3+} and Li^+ co-doped magnesium borate glass ceramics for optically stimulated luminescence dosimetry. *Journal of Luminescence*, 232, 117847.
11. Clem, J. M., De Angelis, G., Goldhagen, P., & Wilson, J. W. (2004). New calculations of the atmospheric cosmic radiation field – results for neutron spectra. *Radiation Protection Dosimetry*, 110(1–4), 423–428.
12. Benker, N., Echeverria, E., Olesen, R., Kananen, B., McClory, J., Burak, Y., Adamiv, V., Teslyuk, I., Peterson, G., Bradley, B., Wilson, E. R., Petrosky, J., Dong, B., Kelber, J., Hamblin, J., Doumani, J., Dowben, P. A., & Enders, A. (2019). Possible detection of low energy solar neutrons using boron based materials. *Radiation Measurements*, 129, 106190.
13. Kodaira, S., Yanagida, Y., Koguchi, Y., Kawashima, H., Kitamura, H., Kurano, M., & Ogura, K. (2018). Note: Complementary approach for radiation dosimetry with Ag^+ -activated phosphate glass. *Review of Scientific Instruments*, 89(11), 116106.

14. Luchechko, A., Zhydachevskyy, Y., Maraba, D., Bulur, E., Ubizskii, S., & Kravets, O. (2018). TL and OSL properties of Mn²⁺-doped MgGa₂O₄ phosphor. *Optical Materials*, 78, 502–507.
15. Padlyak, B., Ryba-Romanowki, W., Lisiecki, R., Adamiv, V., Burak, Y., Teslyuk, I., & Banaszak-Piechowska, A. (2010). Optical spectra and luminescence kinetics of the Sm³⁺ and Yb³⁺ centres in the lithium tetraborate glasses. *Optica Applicata*, 40(2), 427–438.
16. Padlyak, B., Ryba-Romanowki, W., Lisiecki, R., Pieprzyk, B., Drzewiecki, A., Adamiv, V., Burak, Y., & Teslyuk, I. (2012). Synthesis and optical spectroscopy of the lithium tetraborate glasses, doped with terbium and dysprosium. *Optica Applicata*, 42(2), 365–379.
17. Padlyak, B. V., Kindrat, I. I., Protsiuk, V. O., & Drzewiecki, A. (2014). Optical spectroscopy of Li₂B₄O₇, CaB₄O₇ and LiCaBO₃ borate glasses doped with europium. *Ukrainian Journal of Physical Optics*, 15(3), 103–117.
18. Kelly, T. D., Petrosky, J. C., McClory, J. W., Adamiv, V. T., Burak, Y. V., Padlyak, B. V., Teslyuk, I. M., Lu, N., Wang, L., Mei, W., & Dowben, P. A. (2014). Rare earth dopant (Nd, Gd, Dy, and Er) hybridization in lithium tetraborate. *Frontiers in Physics*, 2, 31.
19. Kindrat, I. I., Padlyak, B. V., & Drzewiecki, A. (2015). Luminescence properties of the Sm-doped borate glasses. *Journal of Luminescence*, 166, 264–275.
20. Kindrat, I. I., Padlyak, B. V., & Lisiecki, R. (2015). Judd–Ofelt analysis and radiative properties of the Sm³⁺ centres in Li₂B₄O₇, CaB₄O₇, and LiCaBO₃ glasses. *Optical Materials*, 49, 241–248.
21. Padlyak, B. V., Lisiecki, R., & Ryba-Romanowski, W. (2016). Spectroscopy of the Er-doped lithium tetraborate glasses. *Optical Materials*, 54, 126–133.
22. Kindrat, I. I., Padlyak, B. V., Mahlik, S., Kukliński, B., & Kulyk, Y. O. (2016). Spectroscopic properties of the Ce-doped borate glasses. *Optical Materials*, 59, 20–27.
23. Padlyak, B. V., Kindrat, I. I., Lisiecki, R., Adamiv, V. T., & Teslyuk, I. M. (2017). New effective luminescent materials based on the Sm-doped borate glasses. *Advanced Materials Letters*, 8(6), 723–734.
24. Padlyak, B. V., Lisiecki, R., Padlyak, T. B., & Adamiv, V. T. (2018). Spectroscopy of Nd³⁺ luminescence centres in Li₂B₄O₇:Nd, LiCaBO₃:Nd, and CaB₄O₇:Nd glasses. *Journal of Luminescence*, 198, 183–192.
25. Kindrat, I. I., & Padlyak, B. V. (2018). Luminescence properties and quantum efficiency of the Eu-doped borate glasses. *Optical Materials*, 77, 93–103.
26. Kindrat, I. I., Padlyak, B. V., Lisiecki, R., & Adamiv, V. T. (2019). Optical spectroscopy and luminescence properties of a Tm³⁺-doped LiKB₄O₇ glass. *Journal of Non-Crystalline Solids*, 521, 119477.
27. Adamiv, V., Gamernyk, R., & Teslyuk, I. (2017). Formation of silver nanoparticles in Li₂B₄O₇-Ag₂O and Li₂B₄O₇-Gd₂O₃-Ag₂O borate glasses. *Applied Optics*, 56(17), 5068–5072.
28. Padlyak, B. V., Drzewiecki, A., Padlyak, T. B., Adamiv, V. T., & Teslyuk, I. M. (2018). Resonant excited UV luminescence of the Gd³⁺ centres in borate glasses, co-doped with Gd and Ag. *Optical Materials*, 79, 302–309.
29. Kindrat, I. I., Padlyak, B. V., Kukliński, B., Drzewiecki, A., & Adamiv, V. T. (2018). Enhancement of the Eu³⁺ luminescence in Li₂B₄O₇ glasses co-doped with Eu and Ag. *Journal of Luminescence*, 204, 122–129.
30. Kindrat, I. I., Padlyak, B. V., Lisiecki, R., Adamiv, V. T., & Teslyuk, I. M. (2018). Enhancement of the Er³⁺ luminescence in Er–Ag co-doped Li₂B₄O₇ glasses. *Optical Materials*, 85, 238–245.
31. Kindrat, I. I., Padlyak, B. V., Kukliński, B., Drzewiecki, A., & Adamiv, V. T. (2019). Effect of silver co-doping on enhancement of the Sm³⁺ luminescence in lithium tetraborate glass. *Journal of Luminescence*, 213, 290–296.
32. Kindrat, I. I., Padlyak, B. V., Lisiecki, R., & Adamiv, V. T. (2020). Spectroscopic and luminescent properties of the lithium tetraborate glass co-doped with Tm and Ag. *Journal of Luminescence*, 225, 117357.
33. Kindrat, I. I., Padlyak, B. V., Lisiecki, R., & Adamiv, V. T. (2021). Spectroscopic and luminescent properties of the lithium tetraborate glass co-doped with Nd and Ag. *Journal of Alloys and Compounds*, 853, 157321.
34. Kindrat, I. I., Padlyak, B. V., Lisiecki, R., Drzewiecki, A., & Adamiv, V. T. (2022). Effect of silver co-doping on luminescence of the Pr³⁺-doped lithium tetraborate glass. *Journal of Luminescence*, 241, 118468.
35. Kindrat, I. I., Padlyak, B. V., Drzewiecki, A., Adamiv, V. T., Teslyuk, I. M., & Lisiecki, R. (2024). Influence of Ag co-activation on the Dy³⁺ luminescence in lithium tetraborate glasses. *Materials Research Bulletin*, 179, 112979.
36. Padlyak, B. V., Kindrat, I. I., Adamiv, V. T., Kulyk, Y. O., Teslyuk, I. M., Drzewiecki, A., & Stefaniuk, I. (2023). Local structure, spectroscopy and luminescence of the Li₂B₄O₇:Cu,Eu glass. *Materials Research Bulletin*, 167, 112432.
37. Padlyak, B. V., Kindrat, I. I., Adamiv, V. T., Drzewiecki, A., & Stefaniuk, I. (2024). Spectroscopic properties and photoluminescence of the Li₂B₄O₇:Mn,Sm glass. *Materials Research Bulletin*, 175, 112788.
38. Padlyak, B. V., Kindrat, I. I., Adamiv, V. T., Teslyuk, I. M., & Drzewiecki, A. (2024). Spectroscopic properties and luminescence of the lithium tetraborate glasses co-doped with manganese and europium. *Optical Materials*, 154, 115782.
39. Padlyak, B. V., Kindrat, I. I., Drzewiecki, A., & Adamiv, V. T. (2024). Spectroscopic and optical-luminescent properties of the Li₂B₄O₇:Mn,Er glass. *Ukrainian Journal of Physical Optics*, 25(3), 03105–03124.

40. Padlyak, B. V., Kindrat, I. I., Adamiv, V. T., Drzewiecki, A., Cieniek, B., & Stefaniuk, I. (2024). Structural and spectroscopic studies of the lithium tetraborate glass co-doped with Sm and Cu. *Physical Chemistry Chemical Physics*, 26, 22006–22022.
41. Kananen, B. E., Maniego, E. S., Golden, E. M., Giles, N. C., McClory, J. W., Adamiv, V. T., Burak, Y. V., & Halliburton, L. E. (2016). Optically stimulated luminescence (OSL) from Ag-doped $\text{Li}_2\text{B}_4\text{O}_7$ crystals. *Journal of Luminescence*, 177, 190–196.
42. Padlyak, B. V., Mudry, S. I., Kulyk, Y. O., Drzewiecki, A., Adamiv, V. T., Burak, Y. V., & Teslyuk, I. M. (2012). Synthesis and X-ray structural investigation of undoped borate glasses. *Materials Science-Poland*, 30(3), 264–273.

B.V. Padlyak, I.I. Kindrat, K. Szufa, A. Mandowski. (2025). Optically Stimulated Luminescence of the β -Irradiated $\text{Li}_2\text{B}_4\text{O}_7:\text{Cu}, \text{Eu}$ Glass. *Ukrainian Journal of Physical Optics*, 26(3), 03001 – 03010. doi: 10.3116/16091833/Ukr.J.Phys.Opt.2025.03001.

Анотація. Скло $\text{Li}_2\text{B}_4\text{O}_7:\text{Cu}, \text{Eu}$ було досліджене як потенційний активний елемент в дозиметрії оптично стимульованої люмінесценції (ОСЛ). З цією метою було отримано та проаналізовано залежність інтегрального сигналу інфрачервоної ОСЛ (ІЧ-ОСЛ) від дози β -опромінення (β -джерело $^{90}\text{Sr}/^{90}\text{Y}$), а також криві загасання ІЧ-ОСЛ. Було встановлено, що інтенсивність ІЧ-ОСЛ стає сублінійною при дуже високих дозах опромінення, тоді як крива загасання ОСЛ не належить до кінетики першого та другого порядку і описується сумою трьох експоненціальних складових.

Ключові слова: скло $\text{Li}_2\text{B}_4\text{O}_7:\text{Cu}, \text{Eu}$; β -опромінення; оптично стимульована люмінесценція; дозова залежність; крива загасання.